Please cite as: Lei Wang, D. H. Liang, A. F. Crossland, P. C. Taylor, D. Jones and N. S. Wade, "Coordination of Multiple Energy Storage Units in a Low-Voltage Distribution Network," in IEEE Transactions on Smart Grid, vol. 6, no. 6, pp. 2906-2918, Nov. 2015. DOI: 10.1109/TSG.2015.2452579

Coordination of Multiple Energy Storage Units in a Low Voltage Distribution Network

Lei Wang, Daniel H. Liang, *Member IEEE*, Andrew F. Crossland,
Philip C. Taylor, *Senior Member IEEE*, Darren Jones and Neal S. Wade, *Member IEEE*

***Abstract*—A method for the coordination of multiple battery energy storage systems is proposed for voltage control in low voltage distribution networks. The main objective of this method is to solve over-voltage problems with multiple suitably sized energy storage systems. The performance of coordinated control is compared with non-coordinated control using both a Real Time Digital Simulator and a Matlab model of a real UK low voltage distribution network with a high installed capacity of solar photovoltaics. This is used to show that coordinated control is robust and effective at preventing voltage rise problems in low voltage distribution networks. The proposed coordinated control scheme is able to use the BESSs more evenly and therefore reduces the costs of battery replacement to the storage operator in terms of both number of batteries and maintenance visits.**

***Index Terms*—Battery Energy Storage Systems, Coordinated Voltage Control, Distributed Generation, Real Time Digital Simulator, Low Voltage Distribution Network**

I. Introduction

It is anticipated that future low voltage distribution networks (LVDN) will see increasing use of low carbon technologies (LCTs) due to the introduction of carbon taxes that provide incentives for the installation of LCTs in many countries [1]. LCTs, such as photovoltaics (PV), electric vehicles (EV), and heat pumps (HP) are expected to be common technologies, contributing to reduction of greenhouse gas emissions, while increasing energy diversity and security [1].

Although increasing numbers of distributed generators (DGs), such as PV, have had positive effects in helping countries achieve their climate targets, large quantities of PV can pose a significant challenge to conventional distribution networks. For example, large amounts of PV in a network may result in loss of voltage regulation if the existing voltage control cannot respond to fast fluctuation in PV output. Such voltage problems can be either steady state, such as voltage rise and reverse power flow or dynamic, such as power quality issues and reduced reliability [2] [3] [4].

Undervoltage is expected to be caused by the growth of EVs and HPs, particularly at the end of long radial rural LV networks or heavily loaded urban networks [5]. This voltage drop may result in reduced network performance, damage to connected equipment or even restrict growth of LCT.

In future distribution networks, the installation of LCT will cause voltages and power flows to depend more strongly on prevailing meteorological conditions and customer transport and heating behaviour. Network operators cannot refuse installation of LCT and so they will need to design countermeasures to manage any resulting effects on their networks' performance.

Battery energy storage systems (BESS), whether located at the secondary substation or distributed along the feeders, are one smart grid solution that can alleviate the above challenges in LVDN. Other proposed methods include active power curtailment (APC) and demand side response (DSR). APC increases the hosting capacity of distributed generation by reducing PV output when voltage constraints occur [6]. However, this reduces revenue and the amount of renewably generated energy [7]. DSR can also provide voltage control but this requires demand with suitable characteristics [8].

In [9], the benefits of applying BESSs in power systems are analyzed, such as voltage regulation, frequency droop response and power factor correction. In [10], energy storage is seen as one way of implementing peak shaving, voltage control and power flow management. In [11], the authors propose a strategy for voltage support in a distribution network using a BESS. The proposed strategy controls the BESS to export active and reactive power, with reactive power priority. The export of active and reactive power from the energy storage system is optimized for voltage control by using the ratio of voltage sensitivities of active and reactive power export, to minimize the BESS size. In [12], a charging/discharging strategy of locally controlled BESS is proposed to solve voltage excursions.

One challenge to applying multiple energy storage systems in future distribution networks is the creation of a coordinated control strategy [13]. Coordination schemes for DGs have been studied widely in distribution networks. In [14], an energy management algorithm is proposed for coordinating the operation of energy storage and PV generators. In [15], a

This work was supported by Electricity North West, Ltd, and Scottish Power Energy Networks, through Ofgem's innovation funding initiative.

L. Wang, N. S. Wade, and P. C. Taylor are with the School of Electrical and Electronic Engineering, Newcastle University, Newcastle upon Tyne, NE1 7RU, UK (e-mail: n.s.wade@ncl.ac.uk)

D. H. Liang is with DNV GL Singapore 16 Science Park Drive, Singapore118227

A. F. Crossland is with School of Engineering and Computing Sciences, Durham University, Durham, DH1 3LE, UK

D. Jones is with Future Networks at Electricity North West, Ltd, Warrington, WA3 6XG, UK

coordinated voltage control scheme integrating BESS is proposed under unbalanced conditions. The BESS is operated cooperatively with an on-load tap changer (OLTC) to mitigate voltage rise and voltage unbalance problems. However, the proposed method in [15] does not incorporate a coordinated control strategy for multiple energy storage units.

A coordinated strategy based on both decentralized and centralized controllers is developed for managing power output from a group of PVs in a distribution network in [16]. In [17] and [18], optimal power flow (OPF) within a centralized controller is employed for optimising the power exchange of several DGs in the distribution grid. In [19], a coordinated voltage control methodology based on OLTC transformers and distributed BESSs is proposed in order to optimize the operation of an OLTC and realize peak load shaving using energy storage. In [13], a coordinated strategy for multiple energy storage systems is proposed based on centralized and decentralized control for avoiding violation of voltage and thermal constraints.

In this paper, coordinated control of multiple energy storage systems based on voltage sensitivity analysis and a battery aging model is proposed. These calculations give parameters that influence which BESSs are selected to provide strict maintenance of voltage limits. So in this sense, battery aging analysis is included to modify the system's selection behavior in response to battery degradation while consistently maintaining voltage limits. The controller is assessed in a Real Time Digital Simulator (RTDS) for a high resolution, one day study. A separate Matlab model is constructed to reproduce the overall effect of the controller so that multi-year BESS duty cycles can be obtained in reasonable computational time.

This paper is organized as follows: Section II explains the theory of voltage rise, the theory of voltage sensitivity factors, and the differences between centralized and decentralized control; Section III illustrates the proposed coordinated control methodology; Section IV describes a case study application and results are shown in Section V. A discussion is presented in Section VI; and conclusions are drawn in Section VII.

II. Theory of LV voltages and coordinated control

A. *Voltage problems in LVDNs*

Fig. 1 illustrates a single line diagram of a simplified distribution network with a PV generator connected alongside a load. The voltage across this network is expressed as

$$V_{\text{rise}} = V_{\text{PV}} - V_s = \frac{R(P_{\text{PV}} - P_{\text{L}}) + X(Q_{\text{PV}} - Q_{\text{L}})}{V_{\text{PV}}} \quad (1)$$

Where V_s is the substation secondary bus source voltage, V_{PV} is the PV generator voltage, R and X are the feeder line resistance and reactance. P_{PV} and Q_{PV} are the active and reactive power of the PV generation. P_{L} and Q_{L} are the active and reactive power consumed by the load.

Networks, with no distributed generation have unidirectional power flow and voltages decrease along the line. If $P_{\text{PV}} > P_{\text{L}}$ this may cause voltage rise along the feeder. Consequently the network operator needs to consider that the upper voltage limits may be exceeded in networks with PV installed.

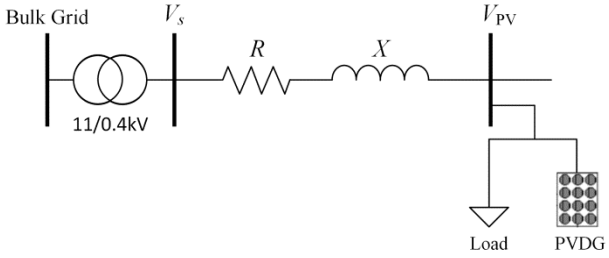

Fig. 1: Two bus distribution system with embedded PV generation

If overvoltage occurs, the network operator can reduce either the cable resistance, R and reactance, X or the reverse power flow in the network, as shown by considering (1). R and X can be reduced by changing the feeder cable. Reverse power can be reduced by increasing the load, P_{L} and Q_{L} The load increase can be achieved by using multiple BESSs distributed within the LVDN to absorb extra power from the network, as identified in [20].

B. *Voltage sensitivity factor*

The voltage sensitivity factor (VSF) describes to what extent the variation in nodal active or reactive power leads to a change in voltage at a specified network location [21][22]. The sensitivities of voltages to the P/Q injections can be determined through the use of a Jacobian matrix [21]. For radial distribution networks, only the voltage magnitude is of interest so the voltage variation, with its sensitivity factor matrix, can be simplified to a compact form [22]. The sensitivity matrix,

$$[\Delta \mathbf{V}] = [\mathbf{VSF}_{\text{P}} \quad \mathbf{VSF}_{\text{Q}}] \begin{bmatrix} \Delta \mathbf{P} \\ \Delta \mathbf{Q} \end{bmatrix}, \quad (2)$$

where $\mathbf{VSF}_{\text{P}} = \partial \mathbf{V}/\partial \mathbf{P}$ and $\mathbf{VSF}_{\text{Q}} = \partial \mathbf{V}/\partial \mathbf{Q}$, is dependent on the network configuration and operating conditions. However, the VSF matrix does not vary significantly with changes in the operating conditions [22], [23].

C. *Decentralized, centralized and coordinated control for multiple energy storage systems*

There are three types of control method to manage the charging/discharging of BESSs: decentralized control, centralized control, and coordinated control.

- In decentralized control, each BESS uses local measurements to control its charging/discharging function. This type of control strategy does not require a wider communication scheme and so is in some respects robust, reliable and cost effective compared to centralized control [6]. However, due to no communication between BESS units, support cannot be received from other BESSs if a unit has reached either an extreme state-of-charge (SoC), a power limit or in the event of complete unit failure.
- In centralized control, the charging and discharging control actions of each BESS unit are determined in a central controller. This approach requires online information of the network state and high computation speed [13]. A significant drawback of this control approach is cost, since it requires a fast, high reliability communications network [13]. In the event of communication failure, each BESS would not be able to respond to a voltage excursion.

- In coordinated control, the control strategy combines the positive features of both centralized and decentralized control [14][16]. The distinctive features of this control are robustness with respect to intermittency and latency of feedback and tolerance to connection and disconnection of network components.

In [13], coordination of multiple energy storage units based on a consensus algorithm for avoiding violation of voltage and thermal constraints is proposed. The consensus algorithm aims to collect energy storage units to work as a coherent group and share the required active power equally among the units. This allows the whole system to survive the failures of some of units. While using this algorithm for network loading management in a centralized controller, a decentralized controller in individual units uses reactive power for voltage support, without considering other units or the wider network. However, since the VSF of each energy storage system is different, this can lead to uneven utilization of energy storage in the network in response to voltage problems. In addition, some LVDN (e.g. urban UK networks [24]) have large amounts of underground LV cables where the R/X ratio is large. In such networks, the effect of reactive power compared with active power is less pronounced when addressing overvoltage.

The new coordinated scheme for multiple BESS in LVDN proposed in this paper is shown in Fig. 2. The centralized controller determines which BESS units are used to address any voltage excursion, whilst the decentralized controller of each BESS uses local measurements to determine specific set points for active and reactive power. The status of each BESS, such as the P/Q power limit, SoC, and energy storage lifetime, is communicated to the centralized controller to update each BESS status within a series of control matrices. The proposed coordinated control method for doing this is described in the following section.

III. Proposed Coordinated Control Method

Two implementations of BESS control have been investigated and compared. In decentralized control, each

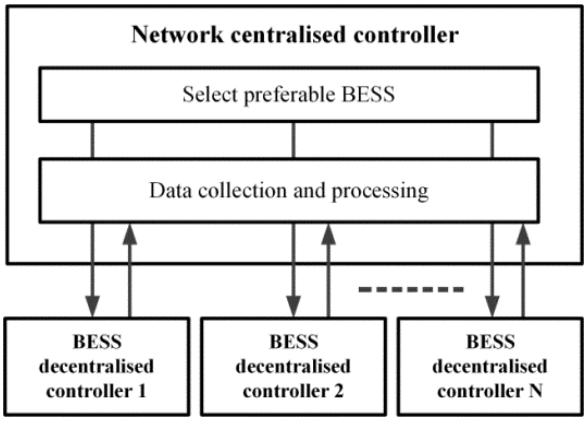

Fig. 2 Overview of proposed coordinated controller containing a centralized controller interacting with several decentralized BESS controllers

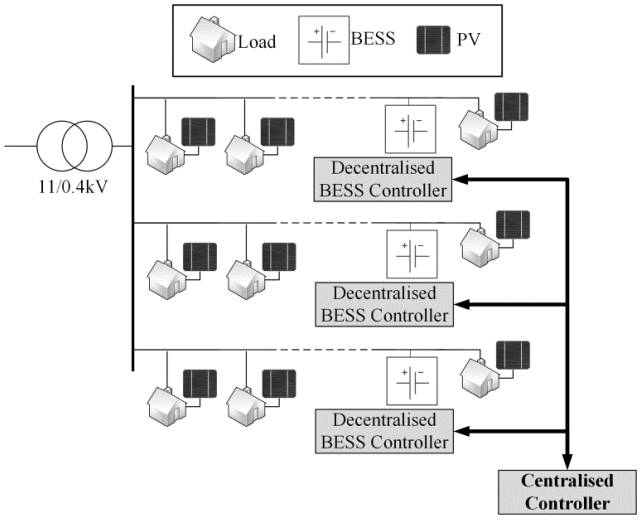

Fig. 3: Coordinated control of multiple energy storage units

BESS uses local measurements of voltage, combined with a VSF, to determine P and Q set points In coordinated control, several BESS units are operated using both a centralized and a decentralized controller as shown in Fig. 3.

The centralized controller determines which BESSs should be used to solve voltage problems by considering the remaining battery cycle life, energy storage availability and their VSF. The selected BESS then determines its individual power set points within its decentralized controller and communicates the results back to the centralized controller for subsequent decision making.

A. *Design of Decentralized Controller*

Under decentralized control, each BESS has visibility only of local measurements. If a voltage excursion happens at this node, the BESS determines its active and reactive power using local network voltage measurements and its VSF. Q is always prioritized above P to preserve the battery SoC as in [25] as this does not use stored energy. While it is noted that changing the ratio of P and Q used by the controller will affect the voltage control performance, this work focuses on coordinated control and strategies to include battery aging models, so evaluation of optimal P/Q ratios is not given here.

Fig. 4 shows the process in which the decentralized controller uses the average phase voltage, V_{ave} and its VSF to calculate active/reactive power to prevent overvoltage. The controller is divided into two parts: a reactive power controller and an active power controller. These two controllers take the actions shown in Table I. These threshold values have been selected and tuned during experimentation, and will change based on the network configuration. Three thresholds are given: upper, V_{uptld} middle, V_{midtld} and lower, V_{lwtld}. Each type of threshold is responsible for different control actions. If V_{ave} is greater than the upper threshold, V_{uptld} a command will set the BESS to charge based on its VSF to solve the overvoltage. Between the middle threshold, and the lower threshold, the charging power is reduced. If the measured voltage drops below the lower threshold, for a pre-defined period of time, the BESS will stop charging as it is no longer needed.

Table I: THRESHOLD VALUES FOR DETERMINING CONTROL ACTION FOR OVERVOLTAGE CONDITION

Battery state and voltage thresholds	Controller action
Voltage at a measured node is greater than upper threshold V_{uptld}	Charge BESS at power based on VSF
BESS charging and voltage drops between middle threshold V_{midtld} and lower threshold V_{lwtld} for time constant	Reduce BESS charge power based on VSF
BESS charging and voltage drops below lower threshold, V_{lwtld} for time constant	Stop charging BESS

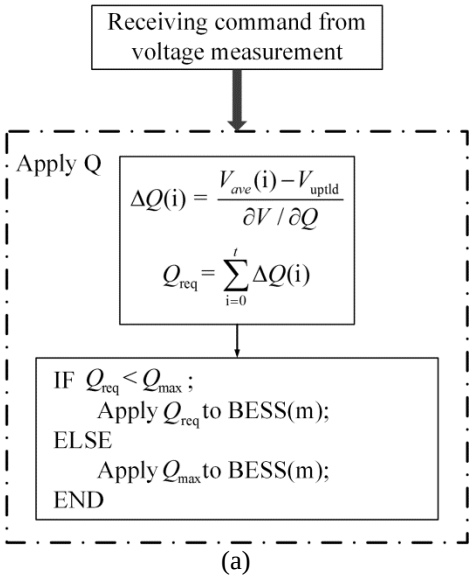

(a)

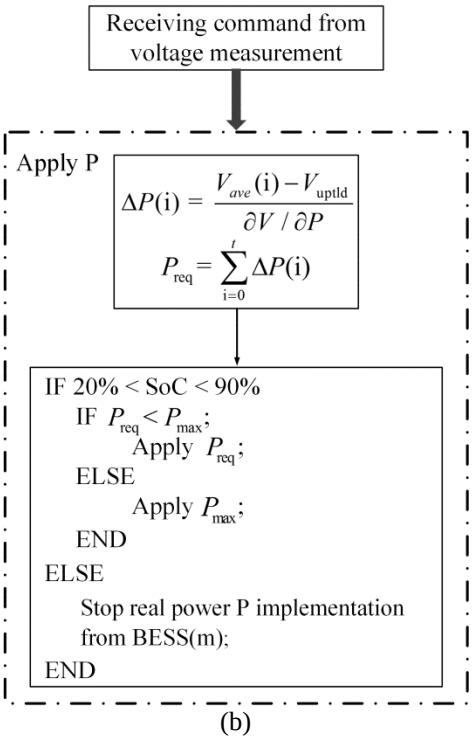

(b)

Fig. 4: Proposed decentralized controller of BESS; (a) Q-operation (b) P-operation

1) Decentralized Reactive Power Controller

Each BESS identifies a local voltage excursion. Separate controllers are required to respond to over or undervoltage conditions, the descriptions that follow are for controlling overvoltage, but the same method is applied for undervoltage.

Q is initially applied to solve the voltage problem based on its local voltage sensitivity factor as shown in Fig. 4 box (a) where t is the current time period. The difference between average phase voltage, V_{ave} and upper threshold voltage V_{uptld} are divided by the VSF, to calculate the required reactive power, Q_{req}. If the required reactive power, Q_{req} is less the maximum rated reactive power, $Q_{\max}$ the decentralized controller will apply required reactive power, Q_{req} to solve the voltage problem. Otherwise, the maximum rated reactive power, $Q_{\max}$ is applied.

2) Decentralized Active Power Controller

If the required reactive power reaches its maximum power limit, the BESS active power P is applied, while Q continues at the rated maximum value. The required active power, P_{req} import from each energy storage unit is similarly calculated based upon its VSF and the difference between average phase voltage, V_{ave} and upper threshold voltage, V_{uptld} as shown in Fig. 4 box (b). If the BESS is at its rated maximum power, $P_{\max}$ or if it's SoC is out of its limit the BESS has no further P capability, and the BESS is not able to solve the voltage problem. This can be addressed by increasing the BESS rating/capacity or by coordinating a fleet of BESSs as proposed in this paper.

B. *Design of Centralized Controller*

The centralized controller maintains an operational matrix, **M** to select the preferred BESSs, which considers:

1. The availability of each BESS to import/export active/reactive power based upon its SoC, charge/discharge power and outage condition. This information is contained in the availability matrix **A** which identifies if the preferable BESS is available to use.
2. The preference for choosing each BESS in the network is based upon the remaining cycle life of each unit and the VSF relative to where the voltage problem occurs. This is contained in the nomination matrix, **F** which determines if there is a preferable BESS based on the information provided.

The operational matrix **M** is used to select the preferable BESS to be used for voltage support. It is the product of the availability and nomination matrices and is split into active and reactive parts

$$\begin{bmatrix} \mathbf{M}_{\text{P}} & 0 \\ 0 & \mathbf{M}_{\text{Q}} \end{bmatrix} = \begin{bmatrix} \mathbf{F}_{\text{P}} & 0 \\ 0 & \mathbf{F}_{\text{Q}} \end{bmatrix} \begin{bmatrix} \mathbf{A}_{\text{P}} & 0 \\ 0 & \mathbf{A}_{\text{Q}} \end{bmatrix}. \quad (3)$$

A detailed description of mathematical expressions and relationships between the availability and nomination matrices now follows.

1) Availability Matrix **A**

The diagonal energy storage availability matrix **A** indicates whether the active and reactive power functions of each BESS are available. The matrix is divided into two parts $\mathbf{A}_P$ and $\mathbf{A}_Q$

$$\mathbf{A}_P = \begin{bmatrix} A_{P1} & & 0 \\ & \ddots & \\ 0 & & A_{Pm} \end{bmatrix} \tag{4}$$

and

$$\mathbf{A}_Q = \begin{bmatrix} A_{Q1} & & 0 \\ & \ddots & \\ 0 & & A_{Qm} \end{bmatrix}, \tag{5}$$

where the index m represents number of storage units in the network.

The active power availability matrix $\mathbf{A}_P$ is an $m \times m$ diagonal matrix and is determined by the BESS SoC and its active power rating

$$A_{Pm} = \begin{cases} 1, & \text{SoC} \le 90\% \text{ and } P_{\text{req}} < P_{\max} \\ 0, & \text{otherwise} \end{cases}. \tag{6}$$

If $A_{Pm}=1$, the BESS(m) can be used for charging or discharging active power. Otherwise, $A_{Pm}=0$; if the battery is at the SoC limit, maximum power limit or the BESS has a fault.

The reactive power availability $\mathbf{A}_Q$ is also an $m \times m$ diagonal matrix similarly defined but without a SoC limit

$$A_{Qm} = \begin{cases} 1, & Q_{\text{req}} < Q_{\max} \\ 0, & \text{otherwise} \end{cases} \tag{7}$$

The SoC is not included because the reactive power function is achieved using the BESS converter and does not rely on the finite energy store.

2) Nomination Matrix **F**

The nomination matrix, **F**, is used to determine the preferred BESS to address a voltage excursion problem by considering the VSF and the aging condition

$$\begin{bmatrix} \mathbf{F}_P & 0 \\ 0 & \mathbf{F}_Q \end{bmatrix} = \begin{bmatrix} \mathbf{VSF}_P & 0 \\ 0 & \mathbf{VSF}_Q \end{bmatrix} \begin{bmatrix} \mathbf{L} & 0 \\ 0 & \mathbf{I} \end{bmatrix}, \tag{8}$$

where $\mathbf{F}_P$ represents the active power nomination matrix and $\mathbf{F}_Q$ denotes the reactive power nomination matrix. Both $\mathbf{VSF}_P$ and $\mathbf{VSF}_Q$ are the sensitivity factors in an $n \times m$ dimensional matrix for n voltage measurement locations in a distribution network and m storage units.

The second term in (8) represents the remaining cycle life, **L**, of each BESS. The age matrix **L** is an $m \times m$ dimension matrix

$$\mathbf{L} = \begin{bmatrix} L_1 & & 0 \\ & \ddots & \\ 0 & & L_m \end{bmatrix}. \tag{9}$$

Reactive power delivery is not affected by the battery aging condition, and so the reactive power nomination matrix $\mathbf{F}_Q$ is only dependent on $\mathbf{VSF}_Q$. As such, an $m \times m$ identity matrix **I** is used.

From the relationship discussed above, both the nomination matrix, **F** and the operational matrix, **M** are $2n \times 2m$ dimension matrices.

The remaining cycle life matrix, **L**, of each BESS is introduced to stop the centralized controller from always nominating the BESS with the highest VSF over other units. Over a BESS project lifetime, total energy passing through the BESSs in the network will increase as BESSs with a lower VSF are used more frequently. However, this shares out the aging of the BESS units so that when the maintenance regime is taken into account the overall project costs can be reduced. The benefit of using an aging model in this way is examined in a case study in section IV and V.

Battery aging is affected by a number of factors such as depth of discharge, number of cycles, temperature etc. and it represents a major component of BESS costs. Decentralized control can focus on one BESS which can cause rapid aging. The coordinated controller offers an opportunity to manage aging rates by distributing usage of the BESSs within the LVDN. In this paper, the remaining cycle life of each BESS is determined using the depth of each daily cycle using a rainflow cycle counter model and a double exponential curve of the form

$$N_{m,t} = \alpha e^{aD_{m,t}} + \beta e^{bD_{m,t}}. \tag{10}$$

This curve is derived for a lead acid battery [26], since this is a well understood technology for storage in LVDN [27]. A number of more complex approaches for battery aging (e.g.[28]) are applicable in this coordinated controller if they provide a value of the deterioration, L_m, of each BESS for the nomination matrix similar to that shown in [12]. However, it is felt that a simple aging model is appropriate for assessing the application of aging management within a coordinated controller.

For each day, this equation relates the number of cycles, $N_{m,t}$ that a battery unit can sustain, to a given depth of discharge, $D_{m,t}$ (expressed as a percentage) using fitting constants α, β, a and b. The Matlab curve fitting tool is used to determine these fitting constants for a suitable valve–regulated lead–acid (VRLA) battery [29] as shown in (11).

$$N_{m,t} = 12500e^{-0.1158D_{m,t}} + 2070e^{-0.01537D_{m,t}}. \tag{11}$$

This has been fitted against the five data points giving cycles to failure at different depths of discharge in the battery manufacturer's datasheet. As can be seen in the datasheet, the trend is distinct and (11) provides a fit to this with a 0.683% root-mean-square error.

The remaining life of each unit is updated in the nomination matrix by the centralized controller at time step T using the expression

$$L_m = 1 - \sum_{t=1}^{T} \frac{1}{N_{m,t}} \tag{12}$$

In addition to the cycle life, batteries also have a calendar life, which for VRLA batteries is typically around 5 years [27]. Extending a BESS's cycle life beyond the calendar life is not advantageous when considering the management of the asset.

C. *Implementation of Coordinated Control Scheme*

Both centralized and decentralized controllers are included in the proposed coordinated control scheme. The centralized controller selects the preferred energy storage unit to be used, whereas the decentralized controller calculates and implements the required active/reactive power set-points. The flowchart in Fig. 5 shows of the steps taken in the coordinated control scheme.

If there is a voltage excursion, voltage rise or drop, the availability matrix $\mathbf{A}_{\mathrm{Q}}$ is first checked from the operational matrix $\mathbf{M}_{\mathrm{Q}}$ (reactive power). If the availability matrix, $\mathbf{A}_{\mathrm{Q}} = 1$ reactive power from the BESS can be applied to solve the voltage problem. The operational matrix $\mathbf{M}_{\mathrm{Q}}$ (reactive power) uses (3) to select the most preferable BESS with the function

$$M_{\mathrm{Q}}^{*} = \arg\max(\mathbf{M}_{\mathrm{Q}}). \tag{13}$$

Once the most preferable BESS is selected, the decentralized controller calculates and implements the required reactive power Q_{req} to support voltage excursion. In addition, the availability matrix $\mathbf{A}_{\mathrm{Q}}$ is updated based on the reactive power output from the BESS converter. If the centralized controller's availability matrix, $\mathbf{A}_{\mathrm{Q}} = 0$ there is no remaining reactive power compensation available in the network, and the centralized controller enters $\mathbf{M}_{\mathrm{P}}$ mode. Q continues at the rated value.

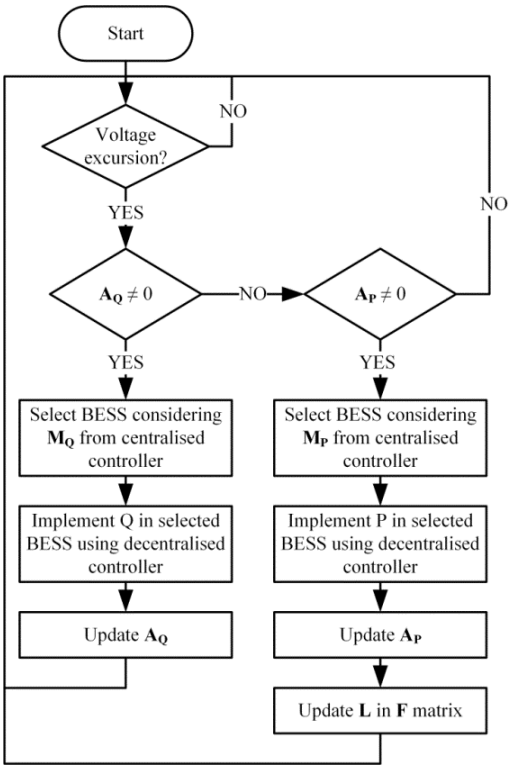

Fig. 5: The main flowchart of proposed coordinated control scheme

Under $\mathbf{M}_{\mathrm{P}}$ operation mode, the active power operation matrix $\mathbf{M}_{\mathrm{P}}$ is checked in the centralized controller. The most preferable and available BESS unit is selected with and the decentralized controller will calculate and implement the required active power P_{req}.

$$M_{\mathrm{P}}^{*} = \arg\max(\mathbf{M}_{\mathrm{P}}) \tag{14}$$

The availability matrix, $\mathbf{A}_{\mathrm{P}}$ and life remaining **L** values for each unit are updated based on P and SoC. In addition, the difference between the required power and maximum rated power will be examined in the decentralized controller. If, for the selected energy storage unit BESS(m), $P_{\mathrm{req}} < P_{\mathrm{max}}$, and SoC is within limits then the decentralized controller communicates with the centralized controller to set the availability $A_p(m) = 1$, otherwise $A_p(m) = 0$ is set. In the case $A_p(m) = 0$, the rated power, P_{rated} from BESS(m) continues at the rated value until it reaches its SoC limit. The centralized controller $\mathbf{M}_{\mathrm{P}}$ will then continue to select the preferable BESS to solve the voltage problem.

IV. Description of Case Study

A. *Network Description and Source Data*

A model of a real radial residential distribution network in Northern England is used in this paper to evaluate the proposed coordinated BESS control scheme. Using maps of the distribution network and technical data provided by a UK distribution network operator, Electricity North West Limited (ENWL), a 4-wire LV model has been developed. One feeder is modelled in detail; it contains 106 domestic loads of which 42 have PV systems as shown in Fig. 6. Each load has an after diversity maximum demand (ADMD) of 1.2 kW, ADMD represents the maximum demand which the electrical distribution network (local transformer) is required to supply, expressed as an average per property. A 3 kW rated PV system is placed on every domestic property with a roof facing ±30° of due south. The position of the secondary transformer LV fixed tap position (1.03 p.u.) is chosen to prevent voltage drop, while maximising the voltage rise headroom in the LV network. The UK regulation on the steady state voltage is applied, in which the customer voltage must be in the range 230 V +10%/−6% [30]. A 2.5 km feeder from the primary substation is included in the model.

A design decision has been taken to make all the units the same size. This standardizes the solution so as to benefit from

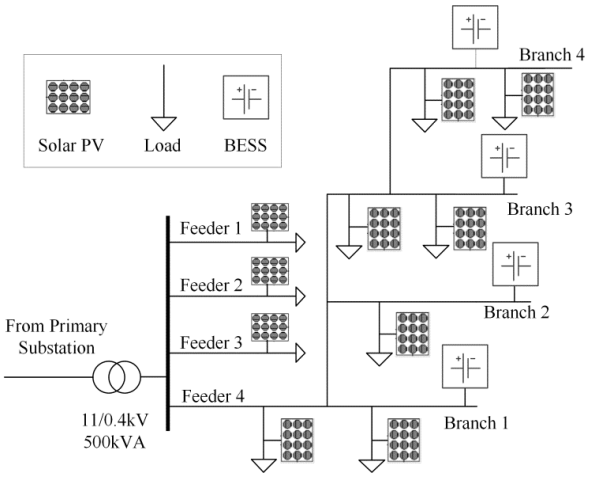

Fig. 6: Benchmark residential urban radial distribution network. There are total 106 residential loads with 42 PV generators in feeder 4

economies of scale in manufacturing. Space is limited in residential LVDNs, so this choice would allow standard installation and maintenance practices to be developed to suit the available space. A decision could be made to encourage installation of storage at customer premises, in which case the adoption of standard procedures would be important. To size and locate the storage units a method developed in previous work was used [31]. This method uses a genetic algorithm to find the optimal locations for the fewest units of storage of a given size to remove all of the overvoltage in a LVDN. This concludes that, under the load and generation conditions investigated in this study, the network can be supported with four identical storage units, each rated at 25 kW/50 kWh.

Reactive power functionality is included to allow minor voltage deviation to be tackled without using the limited energy store. The case study network considered has a relatively high R/X ratio value (3.75—6.25). This means active power is much more effective in mitigating overvoltage. The maximum reactive power drawn from each BESS is therefore limited to 5 kVAr. Doing so also avoids substantially increasing the reactive power being drawn through the secondary transformer which could impact losses and thermal limits in the MV network. Active power from the BESS is used to solve the voltage problem when the applied reactive power resource is insufficient.

B. *Load and Generation Profiles*

In the RTDS model, measured, high resolution irradiance and demand data are used to simulate the network loads and generation. One minute resolution summer day solar irradiance data are taken from a domestic property in Nottinghamshire, UK. The load data has been collected from LV monitoring equipment connected to secondary transformers in the ENWL network. Fig. 7 shows the load profiles and solar irradiance used in the RTDS model.

As shown in Fig. 7, the peak solar irradiance occurs between 9:00—15:00. Voltage rise is most likely to occur during this period. The peak ADMD of 1.2 kW per domestic property occurs in the periods 17:00—20:00.

C. *Simulation Techniques*

Both RTDS models and Matlab/OpenDSS models of the controller have been used. In order to assess the dynamic performance of the proposed coordinated controller, a power electronics model of PV generators and energy storage, based on classical the DQ decoupling control method are needed [32][33]. The RTDS model provides detailed information of real-time performance of these models within one simulation environment. This approach also means that the RTDS model can be interfaced to real devices, allowing power hardware in-the-loop to be used in conjunction with the modelled network.

The Matlab/OpenDSS model evaluates the benefits of the ageing model in the proposed coordinated controller over a ten year period. To do this, standard, one hour resolution, annual irradiance [34] and load profiles [35] are used with a Matlab model of the controller and network.

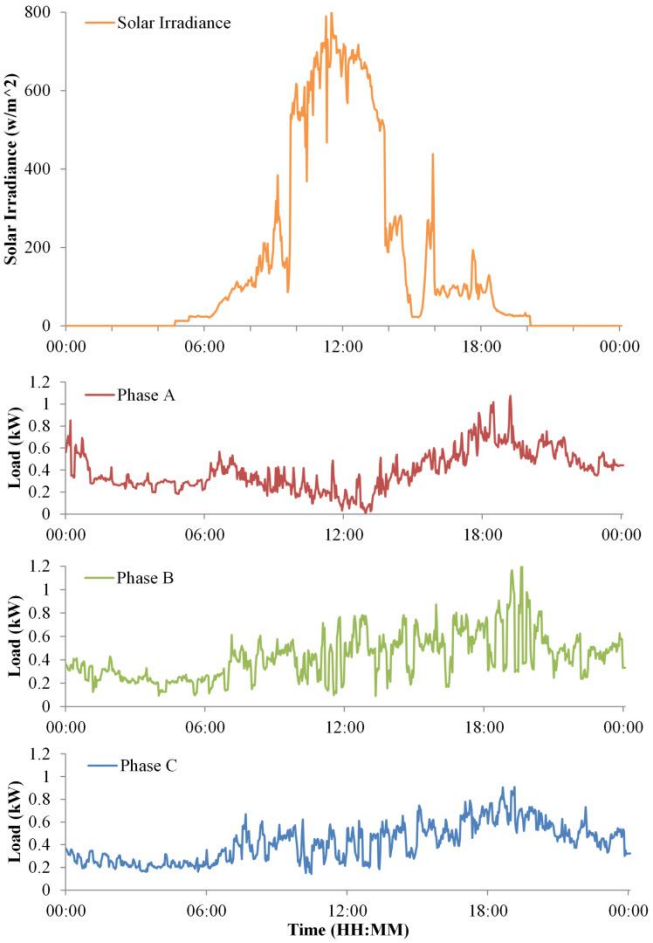

Fig. 7: Solar irradiance and load profiles used in this paper

The Matlab and RTDS models have been compared to ensure their consistency. To do so, the high resolution PV and load profiles shown in Fig. 7 were implemented in both Matlab and RTDS simulation and the results were compared. Fig. 8 shows the comparison for voltages at Branch4; the root mean square error is of the order 0.00415 p.u. Although the Matlab simulation does not run and prove the detailed controller, the overall simulation in terms of SoC and power exchanges that are the same. The two simulation techniques with their

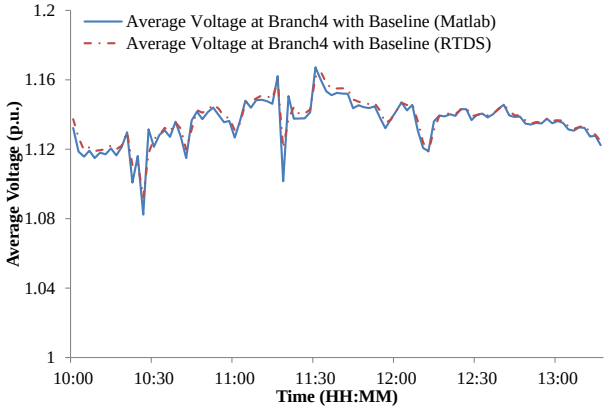

Fig. 8 Comparison between results from Matlab and RTDS simulations

TABLE II SELECTED THRESHOLD AND TIME CONSTANT FOR CASE STUDY

Parameters	Value
Upper Threshold	1.095
Middle Threshold	1.085
Lower Threshold	1.070
Middle Threshold Time Period	30 Seconds
Lower Threshold Time Period	2 minutes

differing time steps and computational burden allow a thorough exploration of the control scheme at different time scales.

Table II shows the thresholds and time constants selected for the decentralized controller of each BESS in the case study. These values have been selected and tuned during experimentation, and will change based on the network configuration.

V. Application of Coordinated Control to Case Study Network

A. *Real time implementation*

The proposed coordinated and non-coordinated control methods are implemented and compared using the RTDS model. Both are compared to a baseline voltage which would occur with no energy storage or curtailment of the PV generation. Note that while the chosen modelling environment provides a 4-wire unbalanced model, the controller as currently conceived takes a single voltage measurement as input. It was chosen to take the average voltage, V_{ave} but it is recognised that other approaches could be taken such as using the most extreme phase voltage. The non-coordinated control method uses the decentralized controller only. Fig. 9(a) illustrates the average of the three phase voltages at branch 4 between 09:00 and 15:00. It can be seen that the baseline average voltage is raised above the limit of 1.10 between 09:40—13:30.

Under the non-coordinated control scenario (with only the decentralized controller), each BESS can only measure and solve its local voltage problem. Fig. 9(a) shows what happens when the charging capacity of BESS4 is reached at 12:30. The average voltage at branch 4 exceeds the limits between 12:30 and 13:20 because the storage cannot absorb any more active power beyond 90% SoC. The average voltage is lowered relative to the baseline by BESSs 1—3 although this is not enough to solve the problem as they are unaware of the excessive voltage at branch 4.

In the case of coordinated control, Fig. 9(a) shows that local overvoltage does not happen as the operational matrix **M** in the centralized controller selects a preferable BESS to solve the average voltage problems when BESS4 reaches its SoC limit. Fig. 9(b) illustrates that BESS4 with coordinated control reaches its SoC limit at 12:20, and the availability of BESS4, $A_P(4) = 0$. The BESS4 is no longer available to support overvoltage at which point other units are used more aggressively.

The voltage profiles with coordinated and non-coordinated control between 11:30—14:00, when voltage rise is most extreme, are shown in Fig. 10(a). Fig. 10(b) and Fig. 10(c) show the power exchange with the non-coordinated and the

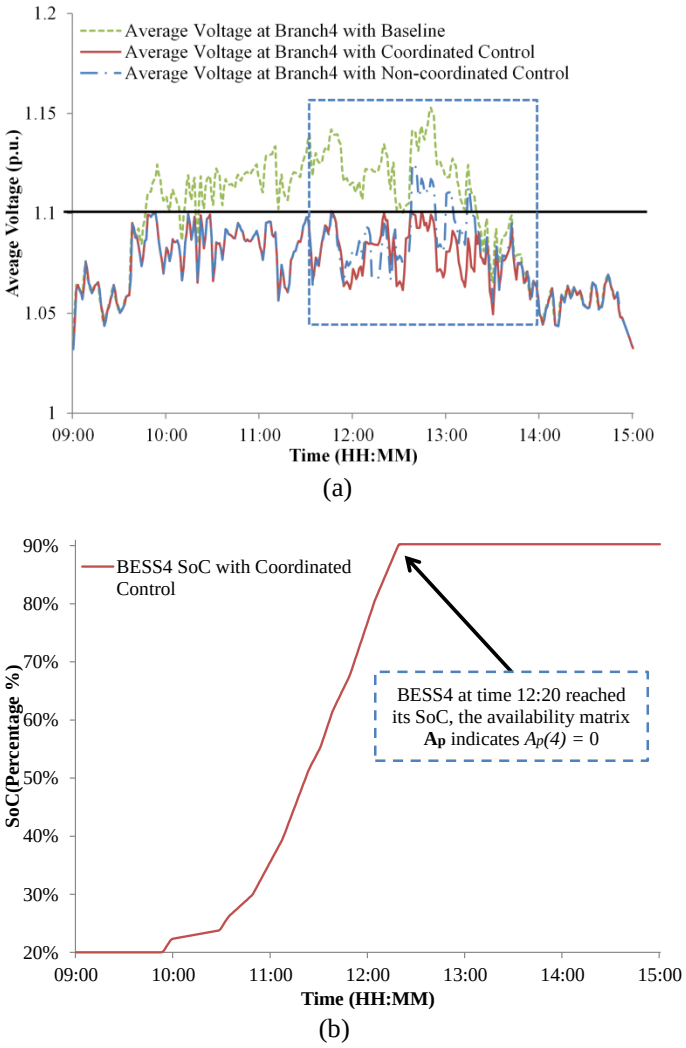

Fig. 9: (a) Average voltage profiles at branch 4 with non-coordinated and coordinated control (b) BESS4 SoC with coordinated control at time between 9:00 and 15:00

coordinated control methods. Under non-coordinated control the BESS has been allowed a higher power rating to demonstrate that if working alone this is required to bring the voltage within limits. With coordinated control, a power of 25 kW is needed from BESS4 to reduce the voltage rise at branch 4 compared to 30 kW with non-coordinated control.

The time sequence of active power exchange with coordinated control and non-coordinated control is summarised as follows:

Between 11:30—12:20, under coordinated control, the centralized controller detects a voltage problem at branch 4 and calls the BESS4 decentralized controller to absorb active and reactive power. However, as the availability matrix $\mathbf{A}_P$ from the centralized controller indicates that the active power capability of BESS4 is insufficient, the operational matrix $\mathbf{M}_P$ in the centralized controller is used to decide the next preferable BESS to solve the voltage rise problem at branch 4. Based on the nomination matrix $\mathbf{F}_P$ and availability matrix $\mathbf{A}_P$, BESS3 is selected to provide additional active power. Fig. 10(d) illustrates the resulting coordination command signal that is

sent to BESS3. The effect of this can be seen in the difference between the charging power of BESS3 in Fig. 10(b) and (c). Between 12:20—13:30, BESS4 reaches its SoC limit of 90%. As shown in Fig. 10(a), the non-coordinated control is unable to solve the voltage problem after 12:20. BESS1-3 do not have visibility of the voltage at branch 4, and therefore do not provide sufficient power (see Fig. 10(b)), to bring the branch 4 voltage within limits.

Conversely, under coordinated control, BESS3 is selected to charge based on the updated operational matrix, $\mathbf{M}_P$ in response to BESS4 being unavailable. Since the required active power from BESS3 is beyond its rated power limits, BESS1 is also selected based upon, $\mathbf{M}_P$ to provide additional active power for branch 4 as shown in Fig. 10(c). The coordination command signal from the operational matrix, $\mathbf{M}_P$ for BESS1 is shown in Fig. 10(e).

Fig. 11 illustrates the active power and SoC of BESS4 operating under coordinated control over a whole day. The energy storage reaches its SoC limit at 12:20. Due to the high charge rate, experiments have shown that to limit the voltage rise without coordinated support from the other units would require an energy capacity of 60 kWh in this case (compared to 50 kWh energy capacity in the case study).

As shown in Fig. 11 for BESS4, the unit is allowed to discharge overnight; this is true of all the BESSs. This increases the voltage within the network, and the power output is set to not cause voltage rise beyond the regulatory limits. It is noted that the BESS could be beneficial if the anticipated future increases in adoption of electric vehicles and heat pumps also cause voltage issues. After charging from PV the BESS can be used to prevent voltage drop by discharging during periods of higher loading.

B. *Asset management*

Assessment of the asset management strategy has been performed by implementing the aging model described in section III in a Matlab/OpenDSS model. The performance of this model is compared to a baseline case with no aging model in the coordinated scheme. If successful, it should more evenly age the BESS units and preferably prevent all of the BESSs from exceeding their cycle life before their calendar life is reached.

Fig. 12 shows the deterioration of the BESSs over a 10 year period under the coordinated control scheme without an aging model implemented (i.e. $\mathbf{L} = \mathbf{I}$). The BESSs reduce in cycle life over the study period as they are charged to manage voltage. The deterioration is much worse (the graph steeper) during the summer months when higher PV output leads to more severe overvoltage. Without the aging model implemented, BESS3 and BESS4 reach the end of the cycle life before the 5 year calendar life is reached. This is because they have a higher VSF than BESS1 and BESS2 relative to where the voltage problem occurs, and are therefore always preferentially selected by the operational matrix $\mathbf{M}$. As a result of this, BESS3 and BESS4 need replacing before their calendar life is reached, which increases the overall replacement costs to the storage operator

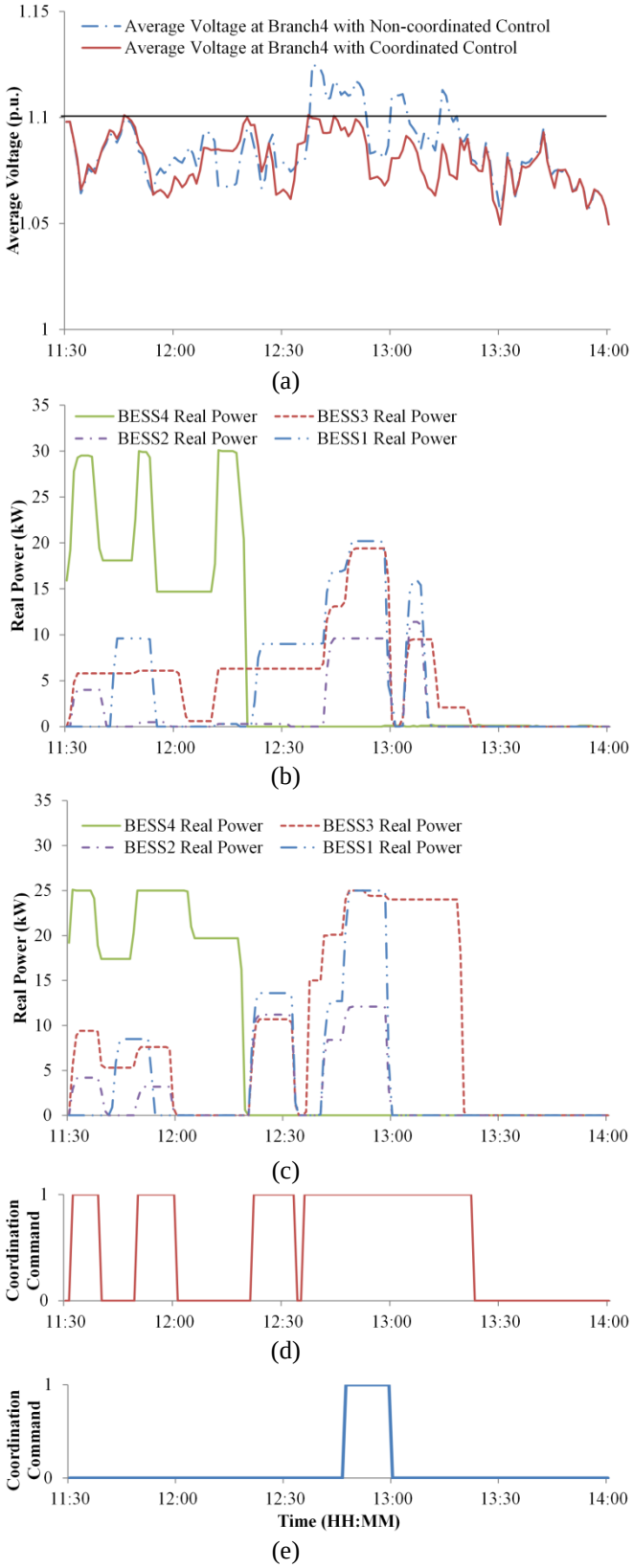

Fig. 10: Performance between 11:30 and 14:00, detailing (a) average voltages at branch 4 under coordinated and non-coordinated control, (b) active power imported to BESSs under non-coordinated control, (c) active power imported to BESSs under coordinated control, (d) coordinated control signal to BESS3 from branch 4 and (e) coordinated control signal to BESS1 from branch 4.

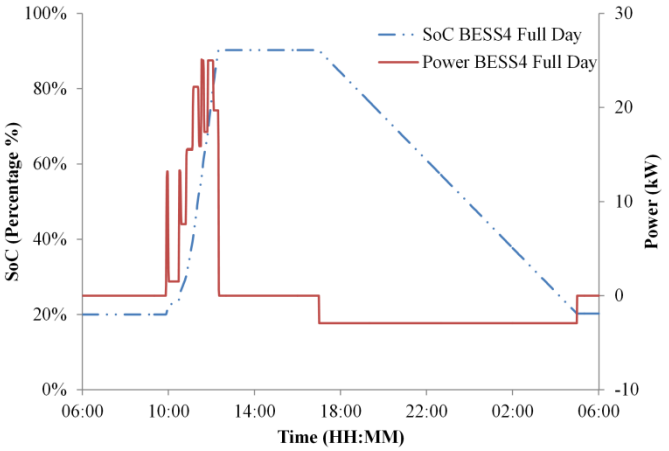

Fig. 11: Active power charged and discharged from BESS4 with its SoC during one whole day

(see Table III). The steepness of the curve of BESS1 contrasts with that of BESS4 which is much shallower due to it being used much less. BESS1 and BESS2 are replaced at the end of their calendar life, but still have cycle life remaining as they are selected less frequently by the operational matrix. In the basecase simulations, six maintenance visits to the network are required, during which the batteries are replaced.

Fig. 13 shows the deterioration of the battery with the aging model implemented. As stated previously, BESS4 is used more frequently in year one as overvoltage occurs most frequently at this location in the LVDN due to the configuration of PV, loads and cables and due to the generation and demand profiles used in this modelling. However, as BESS4 ages, the coordinated controller with the aging model begins to use BESS3, BESS2 then BESS1 more frequently. Due to their lower VSF, BESS1-3 consume more power i.e. the average gradient of the aging graph in Fig. 12 is steeper. There is more even use of the BESS assets and it can be seen that all of the BESSs are replaced only when the calendar life is reached. BESS4 is still needed towards the end of its calendar life, but to a smaller degree than previously as other units are now preferentially selected.

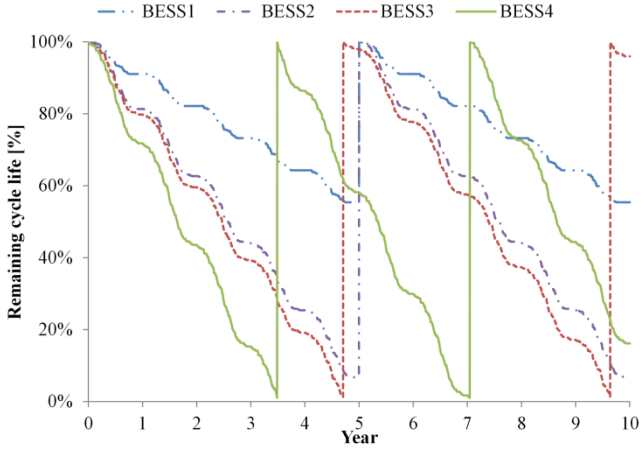

Fig. 12: Remaining cycle life of each BESS without the aging model being implemented in the coordinated controller

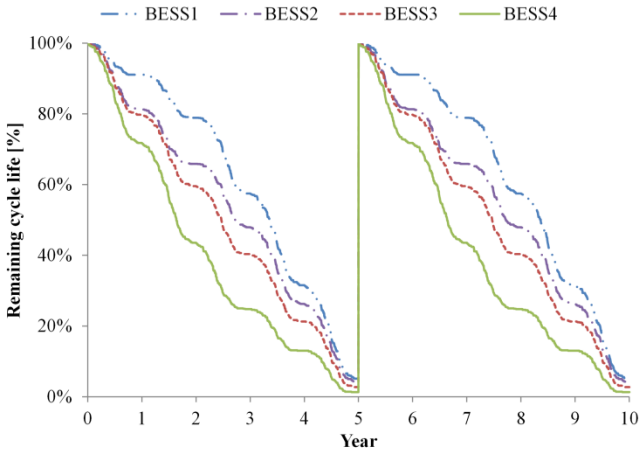

Fig. 13: Remaining cycle life of each BESS with the aging model implemented in the coordinated controller

The aging model has financial benefits by deferring the replacement of BESS3 and BESS4. It can be seen in Table III based on capacity cost of £220/kWh that deferring the replacement of BESS3 and BESS4 saves the network operator £3,489. Furthermore, two maintenance visits to the network to replace batteries are required in comparison to the six visits needed without the aging model which represents further cost saving to the network operator.

Although the aging model reduces replacement costs, it does increase the overall charging energy because it more frequently nominates BESSs which have a lower VSF relative to the location of the voltage problem. This increases the total

TABLE III
COST OF OWNERSHIP WITH AND WITHOUT AGING MODEL

Parameter	No aging model	Aging model	Benefit
BESS capacity cost [£/kWh] [27]	£220		N/A
BESS power cost [£/kW] [27]	£267		
Capital cost of each BESS	£17,675		
Discount rate [36]	6%		
Replacement cost	£95,799	£92,310	£3,489
Maintenance visits per decade	6	2	4

TABLE IV
SUMMARY OF LOSSES WITH AND WITHOUT AGING MODEL WITH 75% EFFICIENT BESSs [27] AND A LOSS INCENTIVE OF £60/MWh [37]

Scenario	No aging model	Aging model	Difference
BESS charging energy [kWh]	175,000	178,000	-3,000
Conversion losses for 75% round trip BESS efficiency [kWh]	43,750	44,500	-750
Cost of losses under UK regulation	£2,625	£2,670	-£45

conversion losses in the BESSs. As shown in Table IV, the aging model causes an additional 750 kWh of loss over ten years which costs the network operator an extra £45 under the UK loss mechanism (£60/MWh [37]). This cost is small compared to the financial saving that the network operator gains from deferring the replacement of BESS3 and BESS4.

VI. Discussion of Results

The method applied in this paper has been shown to be effective in preventing overvoltage in a real LV network that is modelled with a large amount of PV. Non-coordinated and coordinated control methods have been implemented and tested for their ability to prevent overvoltage. The non-coordinated control method works in isolation, using a local voltage measurement and decentralized controller to determine BESS power set-points. By introducing a centralized control unit, the coordinated control also considers the additional factors of BESS aging and SoC to determine which BESS to use and the power set-points. The coordinated approach is shown to require smaller power and energy ratings for the BESS at the network location with the most severe voltage deviations. This results in a lower capital and operating cost in energy storage systems for the storage operator, as can be seen in Table III and IV. Additional costs from implementing a coordinated controller need to be considered to determine the feasibility of a coordinated control project.

The distance between each BESS has a strong influence on the ability of the units to support each other. The closer they are to each other, the greater the ability to support when one unit has failed or reached energy/power limits. However, it may not always be feasible to locate storage unit to close to each other for example due to space constraints or the need to provide support to different parts of an LVDN.

The coordinated control strategy comprises both centralized and decentralized controllers and it is highly dependent on central communication and local measurement systems. In the event of communication failure each unit can operate independently by reverting to non-coordinated control with local measurements. In this eventuality the decentralized controllers at each BESS are not aware of the wider network conditions and so may not be able to solve the most extreme voltage problems on the network.

Because the coordinated control approach allows for cooperative operation, if one of the BESS units fails, other BESS units will automatically be called to improve the voltage at the location of the failed unit. In the case of non-coordinated control, such mitigating measures are not possible.

The decentralized controllers are governed by voltage threshold values that, when combined with voltage sensitivity factors, cause power exchange to adjust up and down. The choice of voltage threshold values is influenced by the network operator's over- and under-voltage tolerance and the ramp rate of changes in solar irradiance. This analysis uses conservative parameters for voltage upper, middle and lower thresholds. However, these values could be tuned to reduce the BESS import and export of both active and reactive power. As the threshold values are narrowed there is a trade-off between the power and energy requirement and the risk of overvoltage.

As further PV systems are added to the network, the location and severity of the voltage excursions may change. By having several BESS operating with a coordinated control strategy, there is a greater potential for this method to adapt to the changing network conditions. In response to the measured voltages across the network, the controller will call on different combinations of BESS to support the voltage. Although the capacity of BESS4 could be increased to remove overvoltage, this investigation has considered a method that uses multiple units with a coordinated controller. By doing so, the proposed storage can adapt to changing generation/demand profile and has a level of robustness to failure of a single BESS i.e. if BESS4 were to fail, there is significant robustness to be able to solve most overvoltage using the other BESS units in this LVDN. The tools provided by this work will enable a thorough investigation of the relationship between the number of units, their location in the network and the resulting robustness as network conditions change with time. The decision to use identically sized BESS units is not necessarily the most effective choice, and this work could be extended by removing this constraint.

The LV secondary transformer fixed tap position was set to prevent under-voltage, in line with the usual practice of network operators. Since voltage deviations were a result of PV generation in these trials, only overvoltage was experienced. However, the coordinated control method can also be adapted to solve under-voltage, occurring under peak load conditions. This might be necessary if electric vehicles and heat pumps are installed, increasing the peak demands on the LVDN.

Although the control method employed has been demonstrated using a UK LVDN, it is inherently applicable to other LV networks.

VII. Conclusion

This paper proposes a scheme for controlling multiple BESSs in an LVDN. This scheme coordinates the power and energy import and export of the BESSs to solve voltage rise caused by PV generation. A real LVDN with measured load profiles and solar irradiance has been used as a case study.

The proposed coordinated control method has been verified using a 24 hour high-resolution implementation in RTDS and a 10 year low-resolution implementation in Matlab. The main advantages of the coordinated control scheme for multiple BESS are as follows:

- By sharing power and energy between the BESSs, the scheme is able to solve real-time voltage problems that cannot be solved with independently controlled BESSs with the same power and energy capacity.
- The rated power and energy of BESS units at the locations with most severe requirements has been reduced, hence the largest unit is smaller when compared with a unit in the same location with non-coordinated control.
- The even sizing of the BESS units offers advantages in maintenance and economy of scale in manufacturing.
- There is greater potential for this proposed method to adapt

to changes in location of extra PV generation, albeit to the limit where extra capacity would then be required. This is not the case with a non-coordinated control.

- The addition of an aging model more evenly utilises the BESSs and consequently reduces the cost of battery replacements for the storage operator, both in terms of battery replacement and maintenance requirements.

The proposed coordinated control can also be adapted for other operational aims, such as peak load shaving and undervoltage.

VIII. Reference

[1] "Low Carbon Technologies - European Commission." [Online]. Available: http://ec.europa.eu/clima/policies/lowcarbon/index_en.htm..

[2] Y.-J. Kim, S.-J. Ahn, P.-I. Hwang, G.-C. Pyo, and S.-I. Moon, "Coordinated Control of a DG and Voltage Control Devices Using a Dynamic Programming Algorithm," *IEEE Trans. Power Syst.*, vol. 28, no. 1, pp. 42–51, Feb. 2013.

[3] A. Canova, L. Giaccone, F. Spertino, and M. Tartaglia, "Electrical Impact of Photovoltaic Plant in Distributed Network," *IEEE Trans. Ind. Appl.*, vol. 45, no. 1, pp. 341–347, 2009.

[4] K. Turitsyn, P. Sulc, S. Backhaus, and M. Chertkov, "Options for Control of Reactive Power by Distributed Photovoltaic Generators," *Proc. IEEE*, vol. 99, no. 6, pp. 1063–1073, Jun. 2011.

[5] Strategies for the uptake of electric vehicles and assoctiated infrastructure. [Online]. Available: https://www.google.co.uk/?gws_rd=cr#bav=on.2,or.r_cp.r_qf.&fp=c3c108cf824f032d&q=Strategies+for+the+uptake+of+electric+vehicles+and+assoctiated+infrastructure. [Accessed: 08-Aug-2013]..

[6] R. Tonkoski, L. A. C. Lopes, and T. H. M. El-Fouly, "Coordinated Active Power Curtailment of Grid Connected PV Inverters for Overvoltage Prevention," *IEEE Trans. Sustain. Energy*, vol. 2, no. 2, pp. 139–147, Apr. 2011.

[7] C.-H. Lin, W.-L. Hsieh, C.-S. Chen, C.-T. Hsu, and T.-T. Ku, "Optimization of Photovoltaic Penetration in Distribution Systems Considering Annual Duration Curve of Solar Irradiation," *IEEE Trans. Power Syst.*, vol. 27, no. 2, pp. 1090–1097, May 2012.

[8] P. Palensky and D. Dietrich, "Demand Side Management: Demand Response, Intelligent Energy Systems, and Smart Loads," *IEEE Trans. Ind. Informatics*, vol. 7, no. 3, pp. 381–388, Aug. 2011.

[9] C. A. Hill, M. C. Such, D. Chen, J. Gonzalez, and W. M. Grady, "Battery Energy Storage for Enabling Integration of Distributed Solar Power Generation," *IEEE Trans. Smart Grid*, vol. 3, no. 2, pp. 850–857, Jun. 2012.

[10] N. S. Wade, P. C. Taylor, P. D. Lang, and P. R. Jones, "Evaluating the benefits of an electrical energy storage system in a future smart grid," *Energy Policy*, vol. 38, no. 11, pp. 7180–7188, Nov. 2010.

[11] M. A. Kashem and G. Ledwich, "Energy requirement for distributed energy resources with battery energy storage for voltage support in three-phase distribution lines," *Electr. Power Syst. Res.*, vol. 77, no. 1, pp. 10–23, Jan. 2007.

[12] M. J. E. Alam, K. M. Muttaqi, and D. Sutanto, "Distributed energy storage for mitigation of voltage-rise impact caused by rooftop solar PV," in *2012 IEEE Power and Energy Society General Meeting*, 2012, pp. 1–8.

[13] G. Mokhtari, G. Nourbakhsh, and A. Ghosh, "Smart Coordination of Energy Storage Units (ESUs) for Voltage and Loading Management in Distribution Networks," *IEEE Trans. Power Syst.*, vol. 28, no. 4, pp. 4812–4820, Nov. 2013.

[14] K. T. Tan, P. L. So, Y. C. Chu, and M. Z. Q. Chen, "Coordinated Control and Energy Management of Distributed Generation Inverters in a Microgrid," *IEEE Trans. Power Deliv.*, vol. 28, no. 2, pp. 704–713, Apr. 2013.

[15] P. Wang, D. H. Liang, J. Yi, P. F. Lyons, P. J. Davison, and P. C. Taylor, "Integrating Electrical Energy Storage Into Coordinated Voltage Control Schemes for Distribution Networks," *IEEE Trans. Smart Grid*, vol. 5, no. 2, pp. 1018–1032, Mar. 2014.

[16] H. Xin, Z. Qu, Z. Lu, D. Gan, and D. Qi, "Cooperative control strategy for multiple photovoltaic generators in distribution networks," *IET Control Theory Appl.*, vol. 5, no. 14, pp. 1617–1629, Sep. 2011.

[17] A. G. Tsikalakis and N. D. Hatziargyriou, "Centralized Control for Optimizing Microgrids Operation," *IEEE Trans. Energy Convers.*, vol. 23, no. 1, pp. 241–248, Mar. 2008.

[18] G. Diaz, C. Gonzalez-Moran, J. Gomez-Aleixandre, and A. Diez, "Complex-Valued State Matrices for Simple Representation of Large Autonomous Microgrids Supplied by *PQ* and *Vf* Generati," *IEEE Trans. Power Syst.*, vol. 24, no. 4, pp. 1720–1730, Nov. 2009.

[19] X. Liu, A. Aichhorn, L. Liu, and H. Li, "Coordinated Control of Distributed Energy Storage System With Tap Changer Transformers for Voltage Rise Mitigation Under High Photovoltaic Penetration," *IEEE Trans. Smart Grid*, vol. 3, no. 2, pp. 897–906, Jun. 2012.

[20] F. Marra, Y. T. Fawzy, T. Bulo, and B. Blazic, "Energy storage options for voltage support in low-voltage grids with high penetration of photovoltaic," in *2012 3rd IEEE PES Innovative Smart Grid Technologies Europe (ISGT Europe)*, 2012, pp. 1–7.

[21] Q. Zhou and J. W. Bialek, "Generation curtailment to manage voltage constraints in distribution networks," *IET Gener. Transm. Distrib.*, vol. 1, no. 3, p. 492, 2007.

[22] M. Brenna, E. De Berardinis, L. Delli Carpini, F. Foiadelli, P. Paulon, P. Petroni, G. Sapienza, G. Scrosati, and D. Zaninelli, "Automatic Distributed Voltage Control Algorithm in Smart Grids Applications," *IEEE Trans. Smart Grid*, vol. 4, no. 2, pp. 877–885, Jun. 2013.

[23] M. A. Kashem and G. Ledwich, "Multiple Distributed Generators for Distribution Feeder Voltage Support," *IEEE Trans. Energy Convers.*, vol. 20, no. 3, pp. 676–684, Sep. 2005.

[24] T. Jiang, G. Putrus, Z. Gao, M. Conti, S. McDonald, and G. Lacey, "Development of a decentralized smart charge controller for electric vehicles," *Int. J. Electr. Power Energy Syst.*, vol. 61, pp. 355–370, Oct. 2014.

[25] M. J. E. Alam, K. M. Muttaqi, and D. Sutanto, "Mitigation of Rooftop Solar PV Impacts and Evening Peak Support by Managing Available Capacity of Distributed Energy Storage Systems," *IEEE Trans. Power Syst.*, vol. 28, no. 4, pp. 3874–3884, Nov. 2013.

[26] H. Bindner, T. Cronin, P. Lundsager, J. F. Manwell, U. Abdulwahid, and I. Baring-gould, *Lifetime Modelling of Lead Acid Batteries*, vol. 1515, no. April. 2005.

[27] S. M. Schoenung and W. V Hassenzahl, "Long- vs . Short-Term Energy Storage Technologies Analysis A Life-Cycle Cost Study A Study for the DOE Energy Storage Systems Program," Albuquerque, NM, 2003.

[28] R. Dufo-López, J. M. Lujano-Rojas, and J. L. Bernal-Agustín, "Comparison of different lead–acid battery lifetime prediction models for use in simulation of stand-alone photovoltaic systems," *Appl. Energy*, vol. 115, pp. 242–253, Feb. 2014.

[29] Deka Solar, "Photovoltaic Batteries," 2012. [Online]. Available: http://www.dekabatteries.com/?pageid=443.

[30] "The Electricity Safety, Quality and Continuity Regulations 2002." [Online]. Available: http://www.legislation.gov.uk/uksi/2002/2665/pdfs/uksi_20022665_en.pdf.

[31] A. F. Crossland, D. Jones, and N. S. Wade, "Planning the location and rating of distributed energy storage in LV networks using a genetic algorithm with simulated annealing," *Int. J. Electr. Power Energy Syst.*, vol. 59, pp. 103–110, Jul. 2014.

[32] "Dynamic performance and control of a static VAr generator using cascade multilevel inverters," *IEEE Trans. Ind. Appl.*, vol. 33, no. 3, pp. 748–755, 1997.

[33] A. Timbus, M. Liserre, R. Teodorescu, P. Rodriguez, and F. Blaabjerg, "Evaluation of Current Controllers for Distributed Power Generation Systems," *IEEE Trans. Power Electron.*, vol. 24, no. 3, pp. 654–664, Mar. 2009.

[34] Solar Radiation Data Manual for Flat-Plate and Concentrating Collectors [Online]. Available: http://rredc.nrel.gov/solar/pubs/redbook/.

[35] Standard Load Profiles [Online]. Available: www.rmdservice.com/guidance/standard_ load_profiles.htm. [Accessed: 05-Nov-2011]

[36] O. Anuta, A. Crossland, D. Jones, and N. Wade, "Regulatory and financial hurdles for the installation of energy storage in UK distribution networks," in *CIRED 2012 Workshop: Integration of Renewables into the Distribution Grid*, 2012, pp. 219–219.

[37] Ofgem, "Electricity Distribution Price Control Review Initial Consultation Document | Ofgem," 2008. .

Lei Wang received MScEng. degree from Curtin University in electrical utility engineering, Perth, Australia in 2011.

He is currently pursuing a Ph.D. degree at Newcastle University in the field of power system engineering examining the use of energy storage on distribution networks. His research interests include renewable energy, and power system dynamics and control.

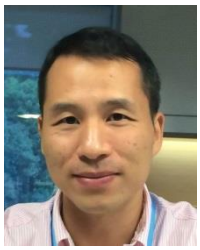

Daniel H. Liang has over 7 years of professional experience in power system engineering. He received his PhD in Nanyang Technological University, Singapore. Throughout his career in industries and academies, Daniel has developed expertise in power network analysis and renewable energy integration. From 2011 to 2013, Daniel worked in Durham University as a senior researcher in Customer Led Network Revolution project (CLNR). He is now a senior smart grid consultant in DNV GL Singapore (former KEMA).

Andrew F. Crossland received a MEng in 2009 in General Engineering with New and Renewable Energy from Durham University, UK, a MSc in Transport and the Environment for the University of Southampton, UK in 2010 and a Ph.D. from Durham University in 2014. His Ph.D compared methods for installing energy storage in LV networks. His present work aims to understand how policy can be designed to support energy storage in the UK and in the management of off-grid power systems in Kenya and Rwanda.

Phil C. Taylor received an Engineering Doctorate in the field of intelligent demand side management techniques from the University of Manchester Institute of Science and Technology (UMIST), Manchester, UK, 2001.

He has industrial experience as an electrical engineer including a period working in the transmission and distribution projects team at GEC Alstom and was Research and Development Director at Econnect (Now Senergy Econnect), a consultancy firm specializing in the grid integration of renewable energy.

Professor Taylor is currently the Director of the Newcastle Institute for Research on Sustainability (NIReS) and Professor of Electrical Power Systems at the School of Electrical and Electronic Engineering, Newcastle University. Professor Taylor is a member of the EPSRC Peer Review College and the CIGRE working group C6.11, "Development and Operation of Active Distribution Networks".

Darren Jones has over 20 years' experience working across the industry in a number of different roles. After gaining a BEng (Hons) in Electrical and Electronic Engineering he spent 7 years at ABB Power T&D based at the Capacitor Division in Ellesmere. This was followed by 7 years at EA Technology initially in Business Development and latterly as manager of the Strategic Technology Programme Substation and Plant Module. His current role at Electricity North West is Research and Development Manager responsible for all aspects of ENWLs portfolio of projects funded under Ofgem's Innovation Funding Incentive. In addition to his day to day role he is also a member of the Energy Networks Association Research and Development and Power Quality and EMC Working Groups and also participates in a number of industry working groups including the current G/DCRP G5/4 Review Group

Neal S. Wade holds a bachelor's degree in electrical engineering and a doctorate degree in physics and has worked in the electronics design and manufacturing industry. In August 2013 he took up a post as Senior Research Associate in the School of Electrical and Electronic Engineering at Newcastle University. Dr Wade works to understand the role for storage and demand response in the distribution system at LV and HV. This is done through real world deployment of energy storage and model based research. He is leading the development of algorithms for optimisation and control of the largest (6MW/10MWh) Li-ion grid connected energy storage system in the UK with UK Power Networks. He leads a broad assessment of the role for energy storage in Electricity North West's distribution network, considering both technical and commercial issues.